J|A|C|S
ARTICLES
Published on Web 08/09/2003

Novel Binding Interactions of the DNA Fragment d(pGpG) Cross-Linked by the Antitumor Active Compound Tetrakis(μ-carboxylato)dirhodium(II,II)

Helen T. Chifotides,*,† Karl M. Koshlap,‡ Lisa M. Pérez,§ and Kim R. Dunbar*,†

Contribution from the Department of Chemistry and the Department of Biochemistry and Biophysics, Texas A&M University, College Station, Texas 77843

Received October 30, 2002; E-mail: chifotides@mail.chem.tamu.edu; dunbar@mail.chem.tamu.edu

Abstract: Insight into the *N7/O6 equatorial* binding interactions of the antitumor active complex $Rh_2(OAc)_4(H_2O)_2$ ($OAc^- = CH_3CO_2^-$) with the nucleotide 5′-GMP and the DNA fragment d(pGpG) has been obtained by one- (1D) and two-dimensional (2D) NMR spectroscopy. The lack of *N7* protonation at low pH values and the significant *increase* in the acidity of *N1−H* ($pK_a \approx 5.6$ as compared to 8.5 for *N7 only* bound platinum adducts), indicated by the pH dependence study of the H8 ^{1}H NMR resonance for the HT *(head-to-tail)* isomer of $Rh_2(OAc)_2(5'\text{-GMP})_2$, are consistent with bidentate *N7/O6* binding of the guanine. The H8 ^{1}H NMR resonance of the HH *(head-to-head)* $Rh_2(OAc)_2(5'\text{-GMP})_2$ isomer, as well as the 5′-G and 3′-G H8 resonances of the $Rh_2(OAc)_2\{d(pGpG)\}$ adduct exhibit pH-independent titration curves, attributable to the added effect of the 5′-phosphate group deprotonation at a pH value similar to that of the *N1* site. The enhancement in the acidity of *N1−H*, with respect to *N7 only* bound metal adducts, afforded by the *O6* binding of the bases to the rhodium centers, has been corroborated by monitoring the pH dependence of the purine C6 and C2 ^{13}C NMR resonances for $Rh_2(OAc)_2(5'\text{-GMP})_2$ and $Rh_2(OAc)_2\{d(pGpG)\}$. The latter studies resulted in pK_a values in good agreement with those derived from the pH-dependent ^{1}H NMR titrations of the H8 resonances. Comparison of the ^{13}C NMR resonances of C6 and C2 for the dirhodium adducts $Rh_2(OAc)_2(5'\text{-GMP})_2$ and $Rh_2(OAc)_2\{d(pGpG)\}$ with the corresponding resonances of the unbound ligands at pH 8.0, showed substantial *downfield* shifts of $\Delta\delta \approx 11.0$ and 6.0 ppm, respectively. The HH arrangement of the bases in the $Rh_2(OAc)_2\{d(pGpG)\}$ adduct is evidenced by intense H8/H8 ROE cross-peaks in the 2D ROESY NMR spectrum. The presence of the terminal 5′-phosphate group in d(pGpG) results in stabilization of *one left-handed* $Rh_2(OAc)_2\{d(pGpG)\}$ HH1 L conformer, due to the steric effect of the 5′-group, favoring left canting in cisplatin-DNA adducts. Complete characterization of the $Rh_2(OAc)_2\{d(pGpG)\}$ adduct revealed notable structural features that resemble those of *cis*-$[Pt(NH_3)_2\{d(pGpG)\}]$; the latter involve repuckering of the 5′-G sugar ring to C3′-endo (N-type) conformation, retention of C2′-endo (S-type) 3′-G sugar ring conformation, and *anti* orientation with respect to the glycosyl bonds. The superposition of the low energy $Rh_2(OAc)_2\{d(pGpG)\}$ conformers, generated by simulated annealing calculations, with the crystal structure of *cis*-$[Pt(NH_3)_2\{d(pGpG)\}]$, reveals remarkable similarities between the adducts; not only are the bases almost completely destacked upon coordination to the metal in both cases, but they are favorably poised to accommodate the *bidentate N7/O6* binding to the dirhodium unit. Unexpectedly, the two metal−metal bonded rhodium centers are capable of engaging in *cis* binding to GG intrastrand sites by establishing *N7/O6* bridges that span the Rh−Rh bond.

Introduction

The activity of the anticancer drug cisplatin {*cis*-$[Pt(NH_3)_2Cl_2]$ *cis*-DDP} has been attributed to its ability to bind to and modify the structure of DNA by forming intrastrand d(GpG) *head-to-head* (HH) cross-links.[1] These platinated sites contribute to a cascade of events, including transcription inhibition and repair shielding of cisplatin-DNA cross-links that lead to cell death.[2] Although a wealth of information is now available for cisplatin-DNA structures,[1] insight into the nature of the GG platinum adducts emerged from the X-ray structure determination of *cis*-DDP bound to d(pGpG)[3] followed by those of longer oligonucleotides.[4,5] The judicious choice of d(pGpG)

* Authors to whom correspondence should be addressed.
† Department of Chemistry, Texas A&M University.
‡ Department of Biochemistry and Biophysics, Texas A&M University.
§ Laboratory for Molecular Simulation, Texas A&M University.

(1) (a) Zamble, D. B.; Lippard, S. J. In *Cisplatin*: *Chemistry and Biochemistry of a Leading Anticancer Drug*; Lippert, B., Ed.; Wiley-VCH: Weinheim, 1999; pp 73−110. (b) Jamieson, E. R.; Lippard, S. J. *Chem. Rev.* **1999**, *99*, 2467−2498. (c) Reedijk, J. *Chem. Rev.* **1999**, *99*, 2499−2510. (d) Cohen, S. M.; Lippard, S. J. *Prog. Nucl. Acid Res. Mol. Biol.* **2001**, *67*, 93−130.

(2) (a) Huang, J.-C.; Zamble, D. B.; Reardon, J. T.; Lippard, S. J.; Sancar, A. *Proc. Natl. Acad. Sci. U.S.A.* **1994**, *91*, 10 394. (b) Zhai, X.; Beckmann, H.; Jantzen, H.-M.; Essigmann, J. M. *Biochemistry*, **1998**, *37*, 16307. (c) Ohndorf, U.-M.; Rould, M. A.; He, Q.; Pabo, C. O.; Lippard, S. J. *Nature* **1999**, *399*, 708. (d) Lee, K.-B.; Wang, D.; Lippard, S. J.; Sharp, P. A. *Proc. Natl. Acad. Sci. U.S.A.* **2002**, *99*, 4239.

(3) (a) Sherman, S. E.; Gibson, D.; Wang, A. H.-J. and Lippard, S. J. *Science*, **1985**, *230*, 412. (b) Sherman, S. E.; Gibson, D.; Wang, A. H.-J. and Lippard, S. J. *J. Am. Chem. Soc.* **1988**, *110*, 7368.

10.1021/ja0291585 CCC: $25.00

Chart 1. Structure and Atom Numbering of (a) Dinucleotide d(pGpG) and (b) Nucleotide 5′-GMP.

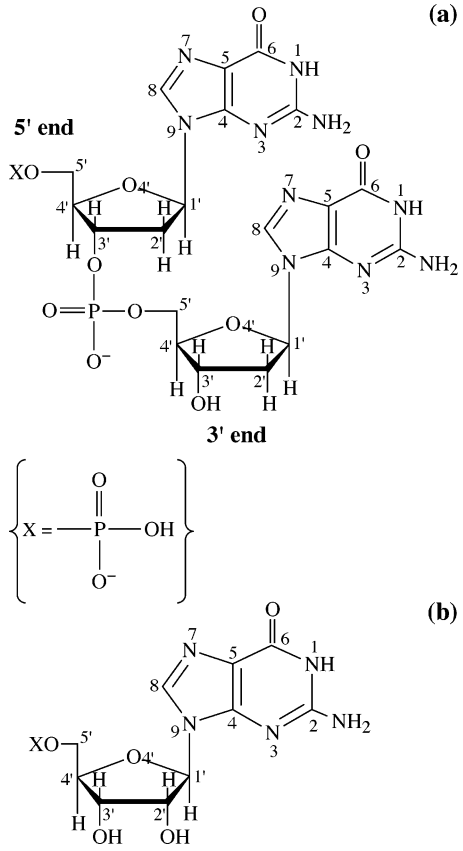

(Chart 1a) to d(GpG) affords the formation of a neutral species upon platination and facilitates important hydrogen bonding interactions that stabilize the complex.[3] Salient features of the d(pGpG) adduct, formed upon *N7* binding of the adjacent guanine bases to *cis*-DDP, include a HH cross-link which results in reduction of the dihedral angle of the bases between ~76° to 87° and destacking of the adjacent residues.[3] The importance of this dinucleotide adduct has been underscored by the recent crystal structure of an HMG (high mobility group) domain/*cis*-DDP modified DNA 16-base pair oligonucleotide complex;[2c] in the latter the dihedral angle between the cisplatin coordinated guanine bases is strikingly similar to the dihedral angle in the *cis*-[Pt(NH$_3$)$_2$\{d(GpG)\}] crystal structure,[3] but considerably larger than that observed in duplexes containing the 1,2-intrastrand d(GpG) cross-link.[2c,5]

In recent years, there has been a resurgence of interest in metal−metal bonded dirhodium compounds with carboxylate ligands in a lantern type structure Rh$_2$(O$_2$CR)$_4$L$_2$ (R = Me, Et, Pr; L = solvent)[6] (Chart 2a), due to their anticancer activity attributed to inhibition of DNA replication and protein synthesis.[7] Apart from axial (*ax*) binding of adenine and guanine derivatives to the dirhodium core,[8] an unprecedented *equatorial* (*eq*) bridging interaction of the purines has emerged from our recent studies.[9,10] In particular, the single crystal X-ray crystal-

Chart 2. (a) Structure of Metal−Metal Bonded Dirhodium Compounds with Carboxylate Ligands and (b) Head-to-Head (HH) and Head-to-Tail (HT) Isomers of [Rh$_2$(OAc)$_2$]$^{2+}$ Core.

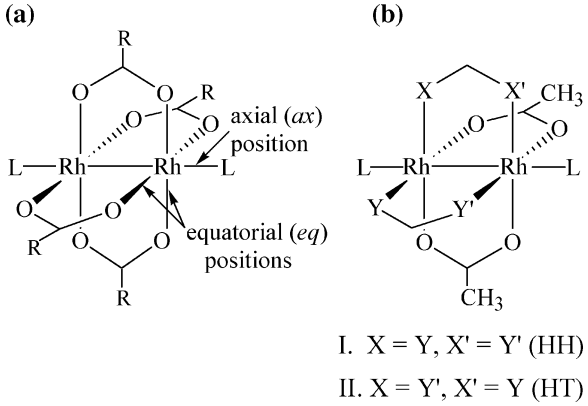

lographic determinations of the adducts with 9-ethylguanine (9-EtGH) have revealed that these bridging modes involve two 9-EtGH groups spanning the dirhodium unit through the *N7*/*O6* sites of 9-EtGH in a *cis* disposition and in a HH (Chart 2b, I) or *head-to-tail* (HT) orientation (Chart 2b, II).[10] The obvious importance of the dirhodium bis-acetate unit bound to tethered guanine bases prompted us to investigate its interactions with the dinucleotide d(GpG),[11] as well as those with GG containing DNA dodecamers.[12] To delineate the effect of the 5′-terminal phosphate group of the d(pGpG) dinucleotide on the conformation of the adduct, we undertook the structural characterization of the Rh$_2$(OAc)$_4$ adducts with 5′-GMP (guanosine-5′-monophosphate) (Chart 1b) and d(pGpG) (Chart 1a) by one- (1D) and two-dimensional (2D) NMR spectroscopy; the structural features of the latter adduct are compared to those of Rh$_2$(OAc)$_2$-\{d(GpG)\}, which are presented in detail in the preceding article of this issue.[11] Moreover, the Rh$_2$(OAc)$_2$\{d(pGpG)\} adduct is compared to that of *cis*-DDP by invoking molecular models. To our knowledge, this is the first study of the DNA fragment d(pGpG) bound to a metal−metal bonded antitumor complex.

(4) Admiraal, G.; van der Veer, J. L.; de Graaff, R. A. G.; den Hartog, J. H. J.; Reedijk, J. *J. Am. Chem. Soc.* **1987**, *109*, 592.
(5) (a) Takahara, P. M.; Rosenzweig, A. C.; Frederick, C. A.; Lippard, S. J. *Nature*, **1995**, *377*, 649. (b) Takahara, P. M.; Frederick, C. A.; Lippard, S. *J. Am. Chem. Soc.* **1996**, *118*, 12 309.
(6) Cotton, F. A.; Walton, R. A. *Multiple Bonds Between Metal Atoms*; Clarendon Press: Oxford, 1993; Chapter 7, pp 431−501.
(7) (a) Erck, A.; Rainen, L.; Whileyman, J.; Chang, I.; Kimball, A. P.; Bear, J. L. *Proc. Soc. Exp. Biol. Med.* **1974**, *145*, 1278. (b) Bear, J. L.; Gray, H. B.; Rainen, L.; Chang, I. M.; Howard, R.; Serio, G.; Kimball, A. P. *Cancer Chemother. Rep. Part I* **1975**, *59*, 611. (c) Howard, R. A.; Spring, T. G.; Bear, J. L. *Cancer Res.* **1976**, *36*, 4402. (d) Erck, A.; Sherwood, E.; Bear, J. L.; Kimball, A. P. *Cancer Res.* **1976**, *36*, 2204. (e) Howard, R. A.; Sherwood, E.; Erck, A.; Kimball, A. P.; Bear, J. L. *J. Med. Chem.* **1977**, *20*, 943. (f) Howard, R. A.; Kimball, A. P. Bear, J. L. *Cancer Res.* **1979**, *39*, 2568. (g) Rao, P. N.; Smith, M. L.; Pathak, S.; Howard, R. A.; Bear, J. L. *J. Nat. Cancer Inst.* **1980**, *64*, 905. (h) Hall, L. M.; Speer, R. J.; Ridgway, H. J. *J. Clin. Hematol. Oncol.* **1980**, *10*, 25. (i) Bear, J. L. In *Precious Metals 1985*: *Proceedings of the Ninth International Precious Metals Conference*; Zysk, E. D.; Bonucci, J. A., Eds.; Int. Precious Metals: Allentown, PA, 1986; pp 337−344.
(8) (a) Aoki, K.; Hoshino, M.; Okada, T.; Yamazaki, H.; Sekizawa, H. *J. Chem. Soc., Chem. Commun.* **1986**, 314. (b) Rubin, J. R.; Haromy, T. P.; Sundaralingam, M. *Acta Crystallogr.* **1991**, *C47*, 1712. (c) Aoki, K.; Salam, M. A. *Inorg. Chim. Acta* **2002**, *339*, 427.
(9) (a) Catalan, K. V.; Mindiola, D. J.; Ward, D. L.; Dunbar, K. R. *Inorg. Chem.* **1997**, *36*, 2458. (b) Catalan, K. V.; Hess, J. S.; Maloney, M. M.; Mindiola, D. J.; Ward, D. L.; Dunbar, K. R. *Inorg. Chem.* **1999**, *38*, 3904.
(10) (a) Dunbar, K. R.; Matonic, J. H.; Saharan, V. P.; Crawford, C. A.; Christou, G. *J. Am. Chem. Soc.* **1994**, *116*, 2201. (b) Crawford, C. A.; Day. E. F.; Saharan, V. P.; Folting, K.; Huffman, J. C.; Dunbar, K. R. and Christou, G. *Chem. Commun.* **1996**, 1113.
(11) Chifotides, H. T.; Koshlap, K. M.; Pérez, L. M.; Dunbar, K. R. *J. Am. Chem. Soc.* **2003**, 125, 10703.
(12) (a) Asara, J. M.; Hess, J. S.; Lozada, E.; Dunbar, K. R.; Allison, J. *J. Am. Chem. Soc.* **2000**, *122*, 8. (b) Chifotides, H. T.; Koomen, J. M.; Kong, M.; Tichy, S. E.; Dunbar, K. R.; Russell, D. H., manuscript in preparation.

Experimental Section

Materials. Guanosine-5′-monophosphate disodium salt monohydrate (5′-GMPNa$_2$·H$_2$O) was purchased from Acros and used without further purification. The dinucleotide d(pGpG) was purchased from Glen Research and used as the lithium salt. Concentrations of the dinucleotide were determined by UV spectroscopy (Shimadzu UV 1601PC spectrophotometer) at 252 nm ($\epsilon_{252} = 2.5 \times 10^4$ M^{-1}cm^{-1}). Deuterium oxide (D$_2$O, 99.996%), deuterium chloride (DCl, 99.5%), sodium deuteroxide (NaOD, 99.5%) and DSS (Sodium 2,2-Dimethyl-2-Silapentane-5-Sulfonate) were purchased from Cambridge Isotope Laboratories. TMP {(CH$_3$O)$_3$PO} was purchased from Aldrich.

Syntheses. Rh$_2$(OAc)$_2$(5′-GMP)$_2$. An aqueous *(aq)* solution (20 mL) of Rh$_2$(OAc)$_4$(H$_2$O)$_2$ (100 mg, 0.21 mmol) was treated with 5′-GMPNa$_2$·H$_2$O (171 mg, 0.42 mmol) dissolved in 5 mL of H$_2$O (pH 8.1). The solution was heated at ∼50 °C for approximately 6−7 days, during which time the color gradually changed to dark green. Small lyophilized aliquots of the reaction solution were monitored by ^{1}H NMR spectroscopy, and the heating was stopped when no unbound 5′-GMP could be detected (monitored by its H8 proton). By the end of the reaction the pH had dropped to 5.6. Samples were copiously lyophilized, prior to preparation for NMR spectroscopy, to remove the acetic acid released during the course of the reaction. MALDI parent ion peak observed at *m*/*z* 1050.

Rh$_2$(OAc)$_2${d(pGpG)}. In a typical reaction, Rh$_2$(OAc)$_4$(H$_2$O)$_2$ (2.5 μmol) in 1 mL of D$_2$O was treated with d(pGpG) (2.5 μmol) in 50 μL of D$_2$O. The pH of the solution after mixing was 7.5. The sample was incubated at 37 °C for several days, and the reaction course was monitored by ^{1}H NMR spectroscopy. By the end of the reaction (∼14 days), the color of the solution had changed to emerald green, and the pH had dropped to 6.0 (lower initial pH values do not have a significant impact on the rate of the reaction). Samples were copiously lyophilized from 99.9% D$_2$O and redissolved in 250 μL of 99.996% D$_2$O for 2D NMR experiments. MALDI parent ion peak observed at *m*/*z* 996 (Figure S6, Supporting Information).

Instrumentation. The 1D ^{1}H NMR spectra were acquired on a 500 MHz Varian Inova spectrometer with a 5 mm switchable probehead. The ^{1}H NMR spectra were typically recorded with 5000 Hz sweep width and 32K data points. Suppression of the residual water peak in D$_2$O spectra was accomplished by presaturation during the recycle delay. The 1D ^{13}C NMR spectra were recorded on a 500 MHz Varian Inova spectrometer operating at 125.76 MHz for ^{13}C, and the 1D ^{31}P NMR spectra were recorded on a Varian 300 MHz spectrometer operating at 121.43 MHz for ^{31}P. The ^{1}H NMR chemical shifts were referenced directly to DSS (Sodium 2,2-Dimethyl-2-Silapentane-5-Sulfonate), whereas the ^{13}C NMR spectra were referenced indirectly to DSS.[13] ^{31}P NMR chemical shifts were referenced to trimethyl phosphate (TMP) (external) at 0 ppm. The 1D NMR data were processed with Varian VNMR 6.1b software.

The 2D NMR data were collected at 5 °C on a Varian Inova 500 MHz spectrometer equipped with a triple-axis gradient penta probe. The homonuclear experiments were performed with a spectral width of ∼5000 Hz in both dimensions. 2D [^{1}H-^{1}H] ROESY (Rotating-frame Overhauser Enhancement SpectroscopY) spectra were collected with mixing times of 150 and 300 ms. A minimum of 2048 points were collected in t_2 with at least 256 points in t_1 and 32−64 scans per increment. 2D [^{1}H−^{1}H] DQF-COSY (Double-Quantum Filtered COrrelation SpectroscopY) spectra, collected with ^{31}P decoupling in both dimensions, resulted in a 1228 × 440 data matrix with 40 scans per increment. 2D [^{1}H−^{31}P] HETCOR (HETeronuclear shift CORrelation) spectra were collected with 2048 points in t_2, 112 points in t_1 with 512 scans per increment. The ^{31}P NMR spectral width was approximately 1500−3500 Hz. All data sets were processed using a 90° phase-shifted sine-bell apodization function and were zero-filled. The baselines were corrected with first or second order polynomials. Two-dimensional (2D) NMR data were processed with nmrPipe.[14]

The pH values of samples were recorded on a Corning pH meter 430 equipped with a MI412 microelectrode probe by Microelectrodes, Inc. The pH dependences of the chemical shifts of several purine nuclei (^{1}H, ^{13}C, ^{31}P) were monitored by adding trace amounts of DCl and NaOD solutions. No correction was applied to the pH values for deuterium isotope effects on the glass electrode.[15] The pH titration curves were fitted to the Henderson−Hasselbalch equation using the program KALEIDAGRAPH,[16] with the assumption that the observed chemical shifts are weighted averages according to the populations of the protonated and deprotonated species.

MALDI (Matrix Assisted Laser Desoprtion Ionization) mass spectra were acquired with an Applied Biosystems Voyager Elite XL mass spectrometer.

Molecular Modeling. Molecular modeling results were obtained using the software package Cerius^2 4.6 (Accelrys Inc., San Diego). The conformational space of each compound was sampled by simulated annealing calculations in the gas phase, performed using the Open Force Field (OFF) program, with a modified version of the Universal Force Field (UFF), as described in the preceding paper of this issue.[11] The 5′-GMP and d(pGpG) adducts have the monoester phosphate group singly protonated (in solution, the second protonation of the 5′-terminal phosphate takes place at pH < 2). In the initial models, the weakly bound *ax* solvent molecules were included with a bond order of 0.1, but it was found that they interact with the 5′-terminal phosphate of the Rh$_2$(OAc)$_2${d(pGpG)} adduct, thus leading to biased conformations; therefore, *ax* solvent molecules have been excluded from all calculations performed in this study.

Results

I. 1D ^{1}H NMR Spectroscopy. a. Rh$_2$(OAc)$_2$(5′-GMP)$_2$. The aromatic region of the ^{1}H NMR spectrum of Rh$_2$(OAc)$_2$(5′-GMP)$_2$ in D$_2$O displays two resonances attributed to the H8 protons of the two possible isomers, HH and HT (Chart 2b). The relative ratio of the H8 resonances for the two isomers is not 1:1, as in the case of 9-EtGH;[10a,11] instead, the ratio is 1:0.8 in favor of the HH isomer (the preference of the HH is highly reproducible). The set of the H8 resonances is accompanied by two upfield resonances at $\delta \approx 2.0$ ppm, in the same ratio, attributable to the methyl groups of the bridging acetate groups. The assignment of each H8 resonance to a particular Rh$_2$(OAc)$_2$(5′-GMP)$_2$ isomer was accomplished by means of 2D ROESY NMR experiments of the reaction mixture solution at pH 7.0;[17] *only* the H8 resonance of the HH isomer reveals a weak cross-peak to the methyl resonance of the bound acetate groups; the 2D NMR data correlate well with the calculated H8/CH$_3$ distance ∼ 5.5 Å for the HH isomer (Table S1). The corresponding distance for the HT isomer is > 6.5 Å, which is a distance that precludes through-space (dipolar) coupling of the relevant protons. The pH-dependent ^{1}H NMR titration curves of the H8 resonances for both Rh$_2$(OAc)$_2$(5′-GMP)$_2$ isomers are depicted in Figure 1; curves A and B correspond to the HH and HT isomers, respectively. The downfield shift of the H8 resonances of the dirhodium adducts with respect to unbound 5′-GMP ($\Delta\delta \approx 0.7$ ppm),[18] and the lack of protonation of *N7* at low pH (Figure 1, curves A and B) corroborate *N7* binding to the rhodium centers.[19,20] For the HT isomer (Figure 1, curve B), the (de)protonation of *N1*−*H* is quite pronounced and the

(13) Markley, J. L.; Bax, A.; Arata, Y.; Hilbers, C. W.; Kaptein, R.; Sykes, B. D.; Wright, P. E.; Wüthrich, K. *Pure Appl. Chem.* **1998**, *70*, 117.
(14) Delaglio, F.; Grzesiek, S.; Vuister, G. W.; Zhu, G.; Pfeifer, J.; Bax, A. *J. Biomol. NMR* **1995**, *6*, 277.
(15) Martin, R. B. *Science*, **1963**, *139*, 1198.
(16) KALEIDAGRAPH, version 3.0.9; Synergy Software: Reading, PA, 1997.
(17) Chifotides, H. T.; Dunbar, K. R., unpublished results.

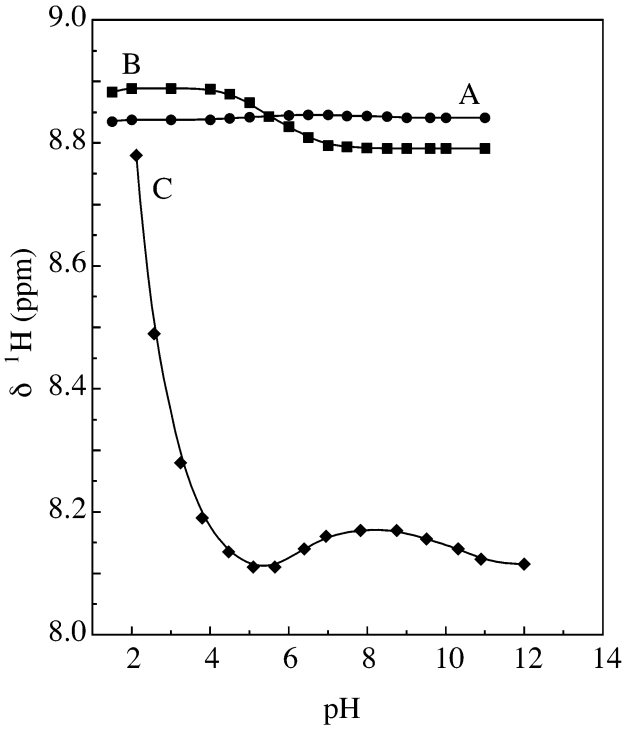

Figure 1. pH dependence of the H8 ^{1}H NMR resonances for (A) HH $Rh_2(OAc)_2(5'\text{-GMP})_2$ (●), (B) HT $Rh_2(OAc)_2(5'\text{-GMP})_2$ (■), and (C) unbound 5′-GMP (◆) in D_2O at 20 °C.

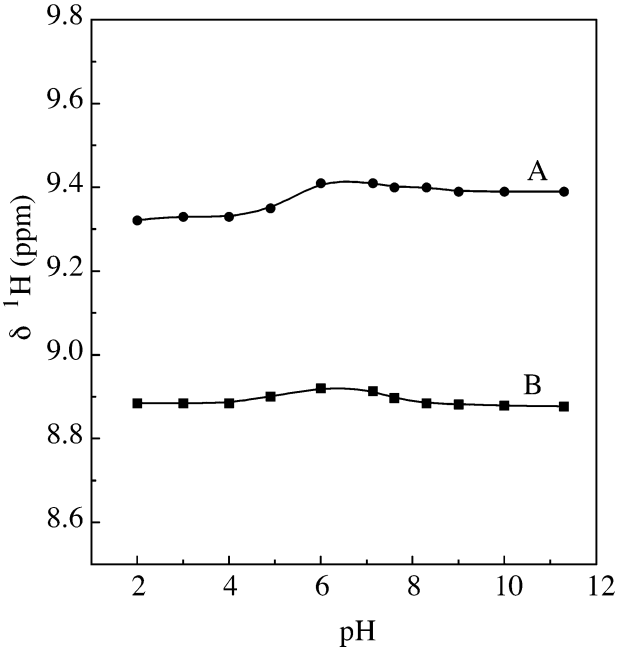

Figure 2. pH dependence of the two H8 ^{1}H NMR resonances for $Rh_2(OAc)_2\{d(pGpG)\}$ (A) 3′-G H8 (●), and (B) 5′-G H8 (■) in D_2O at 20 °C.

inflection point has *decreased* substantially to $pK_a \approx 5.6$, the latter value being comparable to that of *N1*−*H* deprotonation for the 9-EtGH adducts ($pK_a \approx 5.7$);[11] the aforementioned increase in the acidity of the proton attached to *N1* for the 5′-GMP adduct implies *O6* binding to the dirhodium core. In 5′-GMP platinated adducts, the effect of the 5′-phosphate group deprotonation usually causes a ∼0.3 ppm downfield chemical shift change of the H8 proton ($pK_a \approx 6.3$ for unbound 5′-GMP; Figure 1, curve C).[19a,20,21] In the case of the HT $Rh_2(OAc)_2(5'\text{-GMP})_2$ isomer, the effect of (de)protonation of the 5′-phosphate group is not observed (Figure 1, curve B), despite the fact that there is no indication of dephosphorylation of the compound in the pH-dependent ^{31}P NMR titration of the 5′-phosphate group (Figure S1).[19b,22] There is precedent for such an insensitivity of the H8 resonance,[22b] and it is expected in view of the calculated distance between the 5′-phosphate group and the purine H8 for the low energy HT conformers of $Rh_2(OAc)_2(5'\text{-GMP})_2$ (H8···*O*P > 7.0 Å), in contrast to the corresponding distance for the low energy $Rh_2(OAc)_2(5'\text{-GMP})_2$ HH conformers (H8···*O*P ∼ 4.9 Å; Table S1). In particular, plotting the ^{1}H NMR chemical shifts of the H8 for the HH isomer, with respect to pH, gives rise to essentially a straight line (Figure 1, curve A), due to the nearly equal in magnitude, but of opposite directions, effects of the protonations of the 5′-phosphate group and the *N1*−*H* site. The pH dependence study of the 5′-phosphate ^{31}P NMR resonance of the HH $Rh_2(OAc)_2(5'\text{-GMP})_2$ isomer at 20 °C results in $pK_a \approx 5.7$ (Figure S1), the latter value comparing well with the expected $pK_a \approx 5.6$ of *N1*−*H* deprotonation when *O6* participates in binding.[11]

b. $Rh_2(OAc)_2\{d(pGpG)\}$. In the aromatic region of the ^{1}H NMR spectrum of the dirhodium adduct in D_2O at pH 7.8 and 20 °C, the two nonequivalent H8 protons of d(pGpG) give rise to two resonances at $\delta = 9.40$ and 8.89 ppm (Figure S2), downfield shifted from those of the unbound dinucleotide at the same pH ($\delta = 7.98$ and 7.93 ppm), a fact strongly supportive of *N7* binding to the rhodium centers for both guanine bases; the latter is further corroborated by the pH independence of the H8 ^{1}H NMR resonances at pH values near 2 (Figure 2).[19,20,23,24] The two resonances at $\delta = 9.40$ and 8.89 ppm were respectively assigned to the 3′-G and 5′-G H8 protons by analysis of 2D NMR spectroscopic data *(vide infra)*. The two upfield resonances at $\delta = 1.95$ and 1.99 ppm are in 1:1 ratio, in good agreement with the presence of two nonequivalent bridging acetate groups bound to the dirhodium core (Chart 3).

As it is the case for *cis*-$[Pt(NH_3)_2\{d(pGpG)\}]$[20] and other platinum adducts with d{pGpG(pX)} oligonucleotides,[25,26] an effect of the first (de)protonation of the terminal 5′-phosphate group on the 5′-G H8 chemical shift is expected. For the $Rh_2(OAc)_2\{d(pGpG)\}$ adduct, the 5′-G H8 appears to be insensitive

(18) (a) Kong, P. C.; Theophanides, T. *Inorg. Chem.* **1974**, *13*, 1167. (b) Kong, P. C.; Theophanides, T. *Inorg. Chem.* **1974**, *13*, 1981. (c) Marcelis, A. T. M.; Canters, G. W.; Reedijk, J. *Recl. J. R. Neth. Chem. Soc.* **1981**, *100*, 391. (d) Polissiou, M.; Viet, M. T. P.; St-Jacques, M.; Theophanides, T. *Inorg. Chim. Acta* **1985**, *107*, 203.
(19) (a) Dijt, F. J.; Canters, G. W.; den Hartog, J. H. J.; Marcelis, A. T. M.; Reedijk, J. *J. Am. Chem. Soc.* **1984**, *106*, 3644. (b) Miller, S. K.; Marzilli, L. G. *Inorg. Chem.* **1985**, *24*, 2421. (c) Chen, H.; Parkinson, J. A.; Parsons, S.; Coxall, R. A.; Gould, R. O.; Sadler, P. J. *J. Am. Chem. Soc.* **2002**, *124*, 3064.
(20) Girault, J.-P.; Chottard, G.; Lallemand, J.-Y. and Chottard, J.-C. *Biochemistry*, **1982**, *21*, 1352.
(21) (a) Williams, K. M.; Cerasino, L.; Intini, F. P.; Natile, G.; Marzilli, L. G. *Inorg. Chem.* **1998**, *37*, 5260. (b) Ano, S. O.; Intini, F. P. Natile, G.; Marzilli, L. G. *Inorg. Chem.* **1999**, *38*, 2989.
(22) (a) Berners-Price, S. J.; Frey, U.; Ranford, J. D.; Sadler, P. J. *J. Am. Chem. Soc.* **1993**, *115*, 8649. (b) Bloemink, M. J.; Engelking, H.; Karentzopoulos, S.; Krebs, B.; Reedijk, J. *Inorg. Chem.* **1996**, *35*, 619. (c) Liu, Y.; Sivo, M. F.; Natile, G.; Sletten E. *Metal Based Drugs*, **2000**, *7*, 169.
(23) Hartwig, J. F.; Lippard, S. J. *J. Am. Chem. Soc.* **1992**, *114*, 5646.
(24) van der Veer, J. L.; van der Marel, G. A.; van den Elst, H.; Reedijk, J. *Inorg. Chem.* **1987**, *26*, 2272.
(25) Berners-Price, S. J.; Ranford, J. D.; Sadler, P. J. *Inorg. Chem.* **1994**, *33*, 5842.
(26) (a) Spellmeyer Fouts, C.; Marzilli, L. G.; Byrd, R. A.; Summers, M. F.; Zon, G.; Shinozuka, K. *Inorg. Chem.* **1988**, *27*, 366. (b) Bloemink, M. J.; Heetebrij, R. J.; Inagaki, K.; Kidani, Y.; Reedijk, J. *Inorg. Chem.* **1992**, *31*, 4656.

Table 1. ^{13}C NMR Chemical Shifts (δ, ppm) for 5′-GMP, d(pGpG) and Their Dirhodium Bis-acetate Adducts in D_2O at 20 °C

	purine carbon atoms					sugar carbon atoms					acetate carbon atoms	
compound	C6	C2	C4	C8	C5	C1′	C4′	C3′	C2′	C5′	–C=O	–CH_3
5′-GMP[a]	158.93	154.03	151.56	137.59	116.00	86.93	84.52[b]	74.30	70.68	63.59[b]		
$Rh_2(OAc)_2$(5′-GMP)$_2$[a,c]	169.57	159.74	152.51	139.96	118.13	87.80	85.26[b]	75.46	71.19	63.46[b]	192.16	22.33
	168.42	158.70	152.47	139.60	117.98	86.94	85.10[b]	75.27	70.88	63.43[b]	192.14	22.28
$Rh_2(OAc)_2$(5′-GMP)$_2$[c,d]	163.21	154.06	153.74	142.33	117.44	89.09	84.47[b]	75.21	70.58	64.57[b]	193.56	23.15
	163.17	153.82	153.27	142.18	117.05	87.82	84.25[b]	74.71	70.07	64.34[b]	193.31	22.44
d(pGpG)[a]	158.90	153.98	151.32	137.57	116.16	83.46	85.82[e]	77.51[b]	38.86	64.85[b]		
	158.29	153.58	151.05	137.38	115.78	82.97	85.31[b]	70.36	36.76	64.05[b]		
$Rh_2(OAc)_2${d(pGpG)}[a]	170.16	160.40	151.77	137.75	118.22						192.64	22.04
	169.81	159.16	151.47	137.50	117.62	*f*	*f*	*f*	*f*	*f*	192.32	21.96
$Rh_2(OAc)_2${d(pGpG)}[d]	163.62	154.00	153.65	143.14	116.91						193.63	22.77
	163.45	153.71	153.28	142.88	116.71	*f*	*f*	*f*	*f*	*f*	193.32	22.31

[a] pH 8.0. [b] Resonance split into a doublet due to coupling to nuclei ^{31}P of the 5′-terminal phosphate. [c] Values reported for both isomers. [d] pH 4.0. [e] Resonance split into a triplet due to coupling to nuclei ^{31}P of the phosphate mono- and diester groups. [f] 2D HMQC (Heteronuclear Multiple Quantum Coherence) and HMBC (Heteronuclear Multiple Bond Correlation) experiments are necessary for the assignment of the deoxyribose carbon atoms.

Chart 3. Structure and Atom Numbering of $Rh_2(OAc)_2${d(pGpG)}[a]

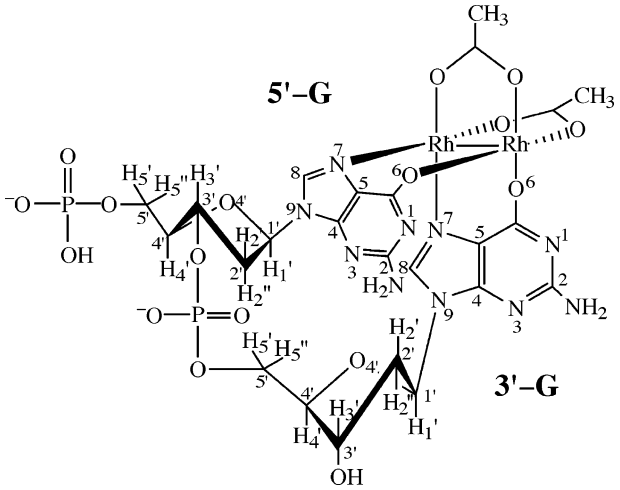

[a] Bond distances are not scaled and angles between atoms are distorted to show structure clearly.

to this effect (Figure 2, curve B); instead, its pH dependence behavior is quite similar to that of the HH isomer of $Rh_2(OAc)_2$-(5′-GMP)$_2$ (Figure 1, curve A); the downfield shift exerted on the H8 resonance, due to the 5′-phosphate deprotonation, is nearly equal in magnitude to the upfield shift due to *N1*−*H* deprotonation, both occurring at p$K_a \approx 5.6$.

The effect of *N1*−*H* deprotonation is not expected to be as pronounced on the 3′-G H8.[20] For the 3′-G H8 of $Rh_2(OAc)_2$-{d(pGpG)}, it is hardly observed (Figure 2, curve A); instead, it appears that the 3′-G H8 resonance is also sensitive to the 5′-phosphate group (de)protonation, indicated by the corresponding downfield chemical shift variation, being small although reproducible, as in the case of *cis*-[Pt(NH_3)$_2$-{d(pGpG)}].[20] This finding is further supported by the calculated distance (3′-G H8···*O*P ∼ 3.0 Å) for the low energy conformers of the adduct (for comparison, 5′-G H8···*O*P ∼ 4.0 Å; Table S1). The substantial decrease in the pK_a value of *N1*−*H* deprotonation to ∼5.6 for $Rh_2(OAc)_2${d(pGpG)}, typical of the 9-EtGH,[11] d(GpG)[11] and 5′-GMP dirhodium adducts, reflects enhanced acidity of the proton attached to *N1* afforded by *O6* binding to the rhodium centers (Chart 3). If *only N7* were bound to the dirhodium core, the pK_a for *N1*−*H* (de)protonation would be expected at 8.5, as in the case of *cis*-[Pt(NH_3)$_2${d(pGpG)}].[20] It is interesting to note that for *O6* methylated guanine bases in d($G^{OMe}pG^{OMe}$), the *N1* protonation is not observed because it is likely to occur below pH 2.0 (where *N7* also becomes protonated), which indicates that *N1* protonation becomes even less favorable when *O6* is methylated instead of metalated.[27]

II. ^{13}C NMR Spectroscopy. ^{13}C NMR spectroscopic data further corroborate guanine *O6* binding to the dirhodium core, and the ensuing increase in the acidity of *N1*−*H*. In Table 1, a compendium of the ^{13}C NMR chemical shift values for 5′-GMP, d(pGpG) and their dirhodium bis-acetate adducts at different pH values is presented. At pH 8.0, *N1* of $Rh_2(OAc)_2$(5′-GMP)$_2$ is deprotonated (Figure 1) (*vide supra)*, and the ^{13}C NMR resonances of C6 for the $Rh_2(OAc)_2$(5′-GMP)$_2$ isomers exhibit a substantial *downfield* shift of $\Delta\delta \approx 11.0$ ppm, whereas the resonances for C2 are downfield shifted by $\Delta\delta \approx 6.0$ ppm with respect to unbound 5′-GMP. The considerable downfield effects on the chemical shifts of C6 and C2 are expected in view of the guanine *O6* binding to the rhodium centers and the increase in the acidity of *N1*−*H* (Figure 1, p$K_a \approx 5.6$).[28] If the ^{13}C NMR chemical shifts of the complexes and the unbound ligand are compared at pH 4.0, *N1* is protonated (Figure 1), and the resonances of C6 are downfield shifted by ∼4.0 ppm, whereas those of C2 remain nearly unaffected.

In reported cases of exclusive *N7* binding of guanosine and inosine nucleos(t)ides to cisplatin, an upfield shift of ∼1−3 ppm on the resonances of C6 and a downfield shift of ∼1−2 ppm on those of C2 have been observed.[18d,28b,29] On the other hand, guanosine or inosine binding to Rh(I) via *O6* induces a 2 ppm upfield shift of the C6 resonance, whereas that of C2 remains unaffected. The same binding mode of the rhodium cation, in the presence of a strong base, induces downfield shifts of ∼6 and 3 ppm for the guanosine C6 and C2 resonances, and ∼7 and 6 ppm for the inosine C6 and C2 resonances, respectively (the ^{13}C NMR resonance of C2 is sensitive to *N1*−*H* deprotonation only, whereas that of C6 is sensitive to *O6* binding as well as *N1*−*H* deprotonation).[28b,c] It is therefore obvious that the $\Delta\delta \approx 11.0$ and 6.0 ppm *downfield* shifts experienced by the C6 and C2 ^{13}C NMR resonances of $Rh_2(OAc)_2$(5′-GMP)$_2$

(27) Struik, A. F.; Zuiderwijk, C. T.; van Boom, J. H.; Elding, L. I.; Reedijk, J. *J. Inorg. Biochem.* **1991**, *44*, 249.
(28) (a) Marzilli, L. G. In *Advances in Inorganic Biochemistry Vol. 3*; *Metal Ions in Genetic Information Transfer*; Eichhorn, G. L., Marzilli, L. G., Eds.; Elsevier: North-Holland, New York, 1981; pp 47−82. (b) Marzilli, L. G.; de Castro, B.; Solorzano, C. *J. Am. Chem. Soc.* **1982**, *104*, 461 and references therein. (c) Abbott, D. W.; Woods, C. *Inorg. Chem.* **1983**, *22*, 1918.
(29) (a) Buncel, E.; Norris, A. R.; Racz, W. J.; Taylor, S. E. *Inorg. Chem.* **1981**, *20*, 98. (b) Barbarella, G.; Bertoluzza, A.; Morelli, M. A.; Tosi, M. R.; Tugnoli, V. *Gazz. Chim. Ital.* **1988**, *118*, 637.

Table 2. ^{1}H and ^{31}P NMR Chemical Shifts (δ, ppm) for $Rh_2(OAc)_2${d(pGpG)} and d(pGpG)

d(GpG) species	G	H8	H1′	$^3J_{H1'-H2'}$/ $^3J_{H1'-H2''}$[a]	H2′	H2″	H3′	H4′	H5′/H5″	base sugar	^{31}P[b] pG-	^{31}P[b] -pG
$Rh_2(OAc)_2${d(pGpG)} HH1 L[c]	5′	8.88	6.23	0/6.4(d)	2.62	2.53	4.52	4.19	4.11/4.40[d]	*anti*	1.00	− 4.38
	3′	9.46	6.23	9.3/5.0(dd)	3.42	2.46	4.72	4.12	3.97/4.00[d]	*anti*		
d(pGpG)[c]	5′	7.95	6.00		2.57[e]	2.57[e]	4.92	4.32	3.81/3.86[d]	*anti*	0.43	− 4.00
	3′	8.00	6.15		2.75	2.44	4.78	4.20	4.13[e]	*anti*		

[a] In Hertz. [b] Relative to TMP (0 ppm). [c] pH 7.8, 5 °C. [d] Not stereospecifically assigned. [e] Overlapped resonances.

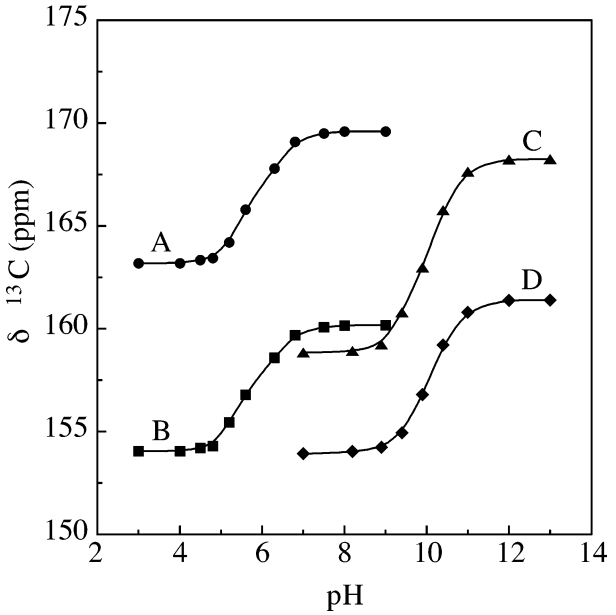

Figure 3. pH dependence of the ^{13}C NMR resonances for (A) (●) C6 of $Rh_2(OAc)_2(5'\text{-GMP})_2$, (B) (■) C2 of $Rh_2(OAc)_2(5'\text{-GMP})_2$, (C) (▲) C6 of unbound 5′-GMP, (D) (◆) C2 of unbound 5′-GMP in D_2O at 20 °C. At each pH value, the ^{13}C NMR chemical shifts of C6 for both $Rh_2(OAc)_2(5'\text{-GMP})_2$ isomers differ by 1 ppm, therefore the titration curves for the second isomer are omitted from the plot; likewise for the ^{13}C NMR chemical shifts of C2.

are attributable to the bidentate *N7/O6* binding and the *N1*−*H* deprotonation of the guanine bases, facts that have been well established by the crystal structure of the HT $Rh_2(OAc)_2(9\text{-EtG})_2$ adduct.[10a] Accordingly, for $Rh_2(OAc)_2${d(pGpG)} at pH 8.0, the C6 and C2 ^{13}C NMR resonances exhibit downfield shifts of $\Delta\delta \approx 11.0$ and 6.0 ppm, respectively, with respect to unbound d(pGpG), which reflect *O6* binding of the guanine bases for the aforementioned compound (an average value for each set of dinucleotide carbon nuclei is given; Table 1). The impact of *N7/O6* binding to the rhodium centers on the NMR spectral properties of the purine, is effectively visualized by plotting the ^{13}C NMR chemical shifts of C6 and C2 for 5′-GMP, d(pGpG) and their dirhodium bis-acetate adducts as a function of pH (Figures 3 and S3). In Figure 3, the titration curves A and B, which correspond to the resonances of C6 and C2 of $Rh_2(OAc)_2(5'\text{-GMP})_2$, respectively, give rise to inflection points at $pK_a \approx 5.7$. This value has decreased significantly from $pK_a \approx 10.0$ for unbound 5′-GMP (Figure 3, curves C, D for C6 and C2, respectively) and is in good agreement with the value for *N1*−*H* (de)protonation ($pK_a \approx 5.6$) derived from the pH-dependent ^{1}H NMR titrations of H8 (*vide supra*; Figure 1, curves A and B). Similar comparisons can be made between $Rh_2(OAc)_2${d(pGpG)} ($pK_a \approx 5.7$; Figure S3; curves A, B for C6 and C2, respectively) and the unbound d(pGpG) ($pK_a \approx 10.0$; Figure S3, curves C and D) at all pH values.

The ^{13}C NMR resonances of C5 for all the dirhodium compounds under study experience only small downfield shifts upon coordination, as has been reported for *O6* bound purines to other metals;[28b] the downfield impact on the ^{13}C NMR resonance of C5 upon *O6* binding may be partially balanced by the expected ∼3 ppm upfield shift (observed in cisplatin adducts), due to *N7* coordination to the metal;[18d,28b,29] the ^{13}C NMR resonance of C8 is usually downfield shifted by ∼3 ppm due to *N7* metal coordination.[18d,29,30] Although this trend is followed by the dirhodium adducts with 5′-GMP (Table 1), the ^{13}C NMR resonances of C8 for the d(pGpG) adduct are not downfield shifted at pH 8.0, as has been noted in a few other cases in the literature.[11,31] For the dirhodium adducts of 5′-GMP and d(pGpG), the ^{13}C NMR chemical shifts for C8 were plotted with respect to pH ($3.0 < pH < 8.0$; the titration curves for C8 have been omitted from the figures for simplicity) giving rise to $pK_a \approx 5.7$ for *N1*−*H* (de)protonation. The observed descending curve without a steep slope for the ^{13}C NMR resonances of C8 is expected, in contrast to those of nuclei C6 and C2, considering that C8 is distal to the (de)protonation position *N1* or the metalation site *O6*.

III. 2D NMR Spectroscopy. 2D ROESY, [^{1}H−^{1}H] DQF-COSY, and [^{1}H−^{31}P] HETCOR NMR spectra were acquired to assign the H8 and sugar proton resonances of the $Rh_2(OAc)_2${d(pGpG)} adduct (Table 2).

$Rh_2(OAc)_2${d(pGpG)}. In the aromatic region of the 2D ROESY NMR spectrum of $Rh_2(OAc)_2${d(pGpG)}, the relatively intense H8/H8 ROE (Rotating frame nuclear Overhauser Effect) cross-peaks (Figure 4) provide definitive evidence that the adduct has HH base orientation (Chart 3) usually observed for the platinum,[32,33] and dirhodium d(GpG)[11] adducts. The two H8 resonances are well separated and downfield shifted (Table 2; $\delta = 8.88$ and 9.46 ppm) from those of the unbound dinucleotide, facts also supporting the HH base orientation (it is well established from the platinum literature that all known HH adducts have at least one relatively downfield H8, whereas HT orientation of the bases gives rise to upfield H8 resonances that have small $\Delta\delta < 0.2$ ppm separation and no H8/H8 ROE cross-peaks).[20,24,25,32−34] The identification of the HH adduct is further supported by the H8−H8 distances derived for the HH and HT

(30) Jia, X.; Zon, G.; Marzilli, L. M. *Inorg. Chem.* **1991**, *30*, 228.
(31) (a) Mukundan, S.; Xu, Y.; Zon, G.; Marzilli, L. G. *J. Am. Chem. Soc.* **1991**, *113*, 3021 and references therein. (b) Marzilli, L. G.; Saad, J. S.; Kuklenyik, Z.; Keating, K. A.; Xu Y. *J. Am. Chem. Soc.* **2001**, *123*, 2764.
(32) (a) Qu, Y.; Bloemink, M. J.; Reedijk, J.; Hambley, T. W.; Farrell, N. *J. Am. Chem. Soc.* **1996**, *118*, 9307. (b) Hambley, T. W.; Ling, E. C. H.; Messerle, B. A. *Inorg. Chem.* **1996**, *35*, 4663.
(33) (a) Ano, S. O.; Intini, F. P.; Natile, G.; Marzilli, L. G. *J. Am. Chem. Soc.* **1998**, *120*, 12 017. (b) Marzilli, L. G.; Ano, S. O.; Intini, F. P.; Natile, G. *J. Am. Chem. Soc.* **1999**, *121*, 9133 and references therein. (c) Williams, K. M.; Cerasino, L.; Natile, G.; Marzilli, L. G. *J. Am. Chem. Soc.* **2000**, *122*, 8021. (d) Sullivan, S. T.; Ciccarese, A.; Fanizzi, F. P.; Marzilli, L. G. *J. Am. Chem. Soc.* **2001**, *123*, 9345 and references therein.
(34) den Hartog, J. H. J.; Altona, C.; Chottard, J. C.; Girault, J. P.; Lallemand, J. Y.; de Leeuw, F. A. A. M.; Marcelis, A. T. M. and Reedijk, J. *Nucleic Acids Res.* **1982**, *10*, 4715.

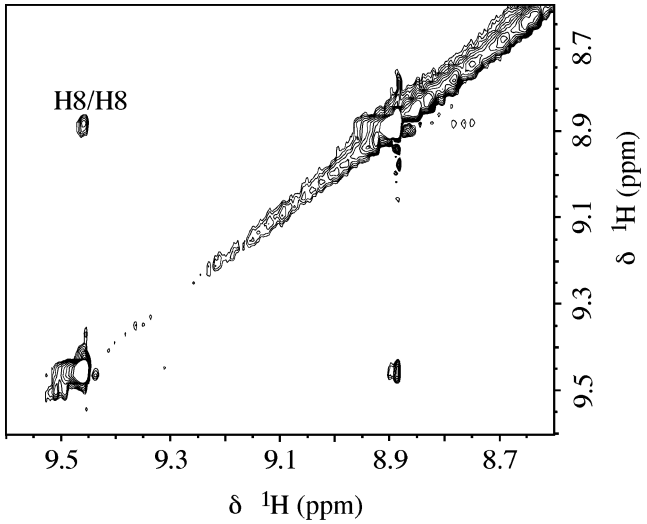

Figure 4. H8/H8 region of the 2D ROESY spectrum of $Rh_2(OAc)_2$-{d(pGpG)} in D_2O at 5 °C, pH 7.8.

models of $Rh_2(OAc)_2${d(pGpG)} presented in the molecular modeling section (*vide infra*). In the HH and HT models, the two H8 atoms are separated by 2.9−3.3 Å and 6.5−6.7 Å, respectively; *only* for the HH models, the distances corroborate the appearance of cross-peaks in the 2D ROESY NMR spectra (ROE intensity between atoms is proportional to the distance between them raised to the inverse sixth power, $\propto r^{-6}$).[35]

The two H8 resonances of $Rh_2(OAc)_2${d(pGpG)} at $\delta = 8.88$ and 9.46 ppm, at pH 7.8 and 5 °C, are assigned to 5′-G and 3′-G, respectively, by assessing the 2D ROESY and [^{1}H−^{1}H] DQF-COSY spectra in conjunction with the [^{1}H−^{31}P] HETCOR NMR spectrum of the adduct. The two ^{31}P NMR resonances at δ = 1.00 and −4.38 ppm are assigned to the phosphate monoester and phosphodiester groups, respectively (Figure 5, panels B and C; typically, the 5′-terminal phosphate resonates downfield from the phosphodiester;[24−26,32a] more details in the ^{31}P NMR section). In the 2D ROESY NMR spectrum, the upfield shifted resonance of the two H8 protons exhibits an H8/H3′ cross-peak and this H3′ has a cross-peak to the phosphodiester ^{31}P NMR resonance in the 2D [^{1}H−^{31}P] HETCOR NMR spectrum (Figure 5, panel B), leading to an unequivocal assignment of the upfield H8 resonance to 5′-G (in a [^{1}H−^{31}P] HETCOR experiment of this type, an H3′−^{31}P diester cross-peak is observed for the 5′-G only, whereas H5′/H5″−^{31}P diester and possibly H4′−^{31}P diester cross-peaks are found for 3′-G).[32a,33d] The assignment of the upfield H8 proton to 5′-G is further corroborated by the [^{1}H−^{1}H] DQF-COSY cross-peak between 5′-G H3′ and its own H4′, which has cross-peaks to H5′/H5″ (Figure 5, panel A); the latter protons give rise to cross-peaks with the terminal 5′-phosphate resonance in the [^{1}H−^{31}P] HETCOR spectrum (Figure 5, panel C). For the 3′-G sugar protons, there are H3′/H4′, H4′/H5′/H5″ cross-peaks in the [^{1}H−^{1}H] DQF-COSY spectrum (Figure 5, panel A); furthermore, 3′-G H5′/H5″ give overlapping cross-peaks with the phosphodiester phosphate in the [^{1}H−^{31}P] HETCOR spectrum (Figure 5, panel B), facts supportive of the previous sugar and H8 assignments. The presence of a very weak H8/H1′ ROE cross-peak for 5′-G H8 along with strong H8/H2′/H2″ and the absence of H8/H1′

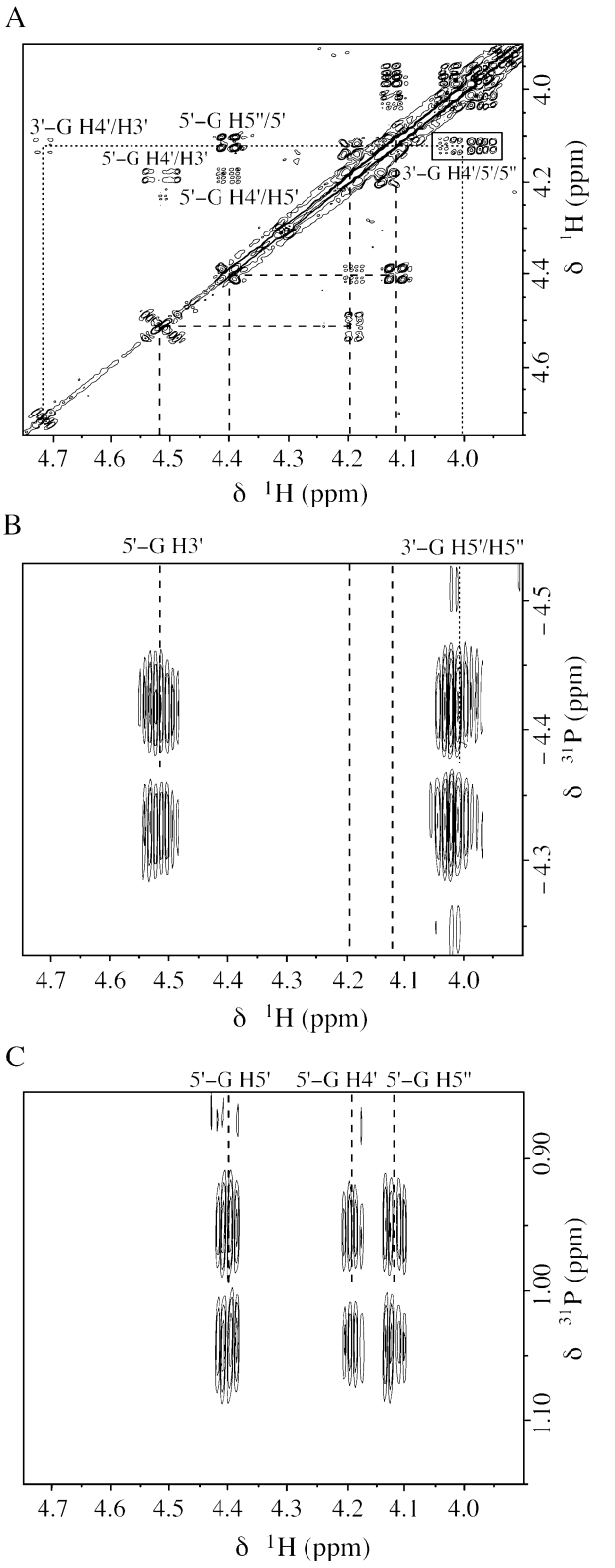

Figure 5. Related regions of the 2D [^{1}H−^{1}H] DQF-COSY and [^{1}H−^{31}P] HETCOR NMR spectra for $Rh_2(OAc)_2${d(pGpG)} in D_2O at 5 °C, pH 7.8; (A) H3′/H4′/H5′/H5″ region of the [^{1}H−^{1}H] DQF-COSY spectrum, (B) phosphate diester {δ (^{31}P) = −4.38 ppm} region, and (C) phosphate monoester (terminal phosphate) {δ (^{31}P) = 1.00 ppm} region of the [^{1}H−^{31}P] HETCOR spectrum; cross-peaks for 5′-G protons are indicated with a medium dash (-------) and those for 3′-G protons with a dotted line (.....). The sugar protons that couple to ^{31}P nuclei are labeled at the top of the [^{1}H−^{31}P] HETCOR spectra (panels B and C); they are traced to the [^{1}H−^{1}H] DQF-COSY spectrum (panel A) with dotted (or dashed) lines.

(35) Derome, A. E. *Modern NMR Techniques for Chemistry Research*, Pergamon Press: 1990, p 106.

Table 3. Summary of Lowest Energy $[Rh_2(OAc)_2]^{2+}$ and *cis*-$[Pt(NH_3)_2]^{2+}$ Adducts with d(pGpG) Derived from Simulated Annealing Calculations

model	energy (kcal/mol)	χ (deg)[a]		P (deg)[b]		5′-G H8/ 3′-G H8 (Å)	3′-G/5′-G dihedral angle (deg)[c]
		5′-G	3′-G	5′-G	3′-G		
$Rh_2(OAc)_2${d(pGpG)} HH1 L[d]	329.5	−134	−45[e]	27	−36	3.12	81.3
$Rh_2(OAc)_2${d(pGpG)} HH R	330.5	−54	−175	−23	−33	3.06	88.5
$Rh_2(OAc)_2${d(pGpG)} HT	335.4	11	−5	20	4	6.62	63.0
cis-[$Pt(NH_3)_2$}d(pGpG)}] HH1 L[f]	295.5	−144	0	30	7	3.52	64.0
cis-[$Pt(NH_3)_2$}d(pGpG)}] HH1 R[f]	296.3	−124	−126	26	−58	2.79	71.8
cis-[$Pt(NH_3)_2$}d(pGpG)}][g]		−89	−110	−8	−43	2.83	80.6

[a] χ = O4′−C1′−N9−C4; $|\chi| > 90°$ and $|\chi| < 90°$ correspond to the *anti* and *syn* range, respectively, for torsion angles $-180° < \chi < +180°$. [b] P = pseudorotation phase angle calculated from the equation $\tan P = ((\nu_4 + \nu_1) - (\nu_3 + \nu_0)/(2\nu_2(\sin 36° + \sin 72°))$($\nu_{0-4}$ are endocyclic sugar torsion angles; $0° \le P \le 36°$ (± 18°) correspond to N sugars, whereas $144° \le P \le 190°$ (± 18°) indicate *S* sugars; $\tan P = \tan(180 + P)$. [c] Dihedral angles between 5′-G and 3′-G were calculated by using atoms N1, N3, and N7 of the purine rings. [d] Conformer experimentally observed. [e] This angle is in the range to be considered *syn*; however, the H8−H2′ distance is less than the H8−H1′ distance and other low-energy structures have χ angles in the *anti* range. [f] In 1:1 ratio with other HH1 conformer in the crystal structure.[3b,45] [g] Crystallographically independent molecule 2 of the asymmetric unit.[3b]

ROE cross-peaks for 3′-G are consistent with the conclusion that both sugar rings are in the *anti* orientation[33] (the *anti/syn* orientation is defined by the χ = O4′−C1′−N9−C4 torsion angle and pertains to the position of the sugar relative to the base)[36] typically observed in *cis*-[PtA_2(dinucleotide)] complexes.[24,32a,33d,34] The strong H8/H3′ ROE cross-peak along with strong H1′−H2″ (and no H1′−H2′) DQF-COSY peaks imply C3′-endo (N-type) sugar conformation for 5′-G (Chart 3);[33b,37] these findings are further corroborated by the doublet coupling pattern of H1′ ($^3J_{H1'-H2'} = 0$, Table 2) in the [^{1}H−^{1}H] DQF-COSY spectrum (Figure S4; this pattern could not be observed in the 1D ^{1}H NMR spectrum because the two H1′ resonances are overlapped) typical of N-type conformation for deoxyribose sugars.[11,24,32a,33b,34,38] On the contrary, the 3′-G sugar ring retains the C2′-endo (S-type) conformation encountered in B-DNA; this is implied by the appearance of a strong H1′−H2′ DQF-COSY cross-peak along with the doublet of doublets coupling pattern for the H1′ resonance[33] (Figure S4). The retention of the C2′-endo conformation by the 3′-G sugar rings and the repuckering to C3′-endo of the 5′-G sugar rings are features commonly encountered in HH cross-linked platinum dinucleotide adducts.

IV. ^{31}P NMR Spectroscopy. $Rh_2(OAc)_2${d(pGpG)}. In the 1D ^{31}P NMR spectrum, the two resonances at δ = 1.00 and −4.38 ppm are assigned to the phosphate monoester and phosphodiester groups, respectively (Table 2). Typically, the 5′-terminal phosphate resonates downfield from the phosphodiester.[24−26,32a] For $Rh_2(OAc)_2${d(pGpG)}, the phosphate monoester is *downfield* shifted, in agreement with the downfield shift of the 5′-terminal phosphate in reported d(pGpG)[25,26b] and d(pGpGpG)[24] platinum adducts, whereas the phosphate diester is *upfield* shifted from the corresponding resonances of the unbound d(pGpG). Usually, upfield shifted resonances of the dinucleotide phosphodiester group are observed in HT isomers;[33b,c] the dirhodium adduct has the HH conformation (*vide infra*), therefore the latter reason is not applicable. An upfield shift has been observed for the dinuclear (Pt, Pt) chelate adduct [{*trans*-$PtCl(NH_3)_2$}$_2${μ-$H_2N(CH_2)_3NH_2$}{d(GpG)}].[32a] Moreover, upfield shifted ^{31}P NMR resonances have been observed for *trans*-[$Pt(NH_3)_2Cl_2$] with d(GTG)[39] and for a hairpin-like structure of cisplatin with d(TCTCGGTCTC).[40] A number of factors not well understood may lead to these upfield ^{31}P NMR shifts; for DNA adducts, one plausible explanation is hydrogen bonding between the diester phosphate and amino groups[25] (in this case the exocyclic amino group of the 3′-G for which the measured distance to the diester phosphate in the models is ∼4.0 Å). To assess such possible interactions, the temperature dependence study of the phosphate monoester and diester ^{31}P NMR resonances for $Rh_2(OAc)_2${d(pGpG)} was considered; from the relevant plot (Figure S5), it is obvious that there is negligible temperature effect on the 5′-terminal phosphate ^{31}P NMR resonance, but there is linear temperature dependence of the phosphodiester ^{31}P NMR resonance, an indication of intramolecular effects on that group.[41]

V. Molecular Modeling. Models of the dirhodium adducts were constructed and subjected to simulated annealing calculations. Conformational features determined by NMR spectroscopy are reproduced well by the calculations.

Despite the fact that the two $Rh_2(OAc)_2(9\text{-EtG})_2$ isomers are isoenergetic, in agreement with their 1:1 ratio in solution (inferred from ^{1}H NMR spectroscopy),[11] the $Rh_2(OAc)_2(5'\text{-GMP})_2$ HH isomer is favored over the HT by 3 kcal/mol (Table S2) (initial structures included combinations of *anti* and *syn* sugar orientations for both isomers). The qualitative energy difference of the two isomers concurs with the experimental 1:0.8 ratio favoring the HH isomer *(vide supra)*, although it is rather high as compared to the energy difference between the d(pGpG) HH and HT dirhodium adducts (Table 3). Close examination of the HH and HT models suggests that sugar and phosphate nonbonding interactions, which are present in the HH isomer only, render it preferable. To evaluate the contribution of the latter interactions to the stability of the HH isomer, the dirhodium guanosine models $Rh_2(OAc)_2(5'\text{-Guo})_2$ were constructed; an energy difference of 1.3 kcal/mol is obtained in favor of the HH isomer. It is therefore likely that the interactions of the N9 purine substituent are the driving force for the slight preference of the $Rh_2(OAc)_2(5'\text{-GMP})_2$ HH isomer (in the case of the platinum adducts, the HT isomers dominate due to favored dipole base−base interactions).[42,43] Various distances listed in Table S1 corroborate well the ^{1}H NMR pH dependence data presented in the foregoing sections. Similarly, HH and HT structures for $Rh_2(OAc)_2${d(pGpG)} were considered. The H8−H8 distances in the HH conformers (Table 3) support the

(36) Saenger, W. In *Principles of Nucleic Acid Structure*; Cantor, C. R., Ed.; Springer-Verlag: New York, 1984; pp 1−158.
(37) Widmer, H.; Wüthrich, K. *J. Magn. Reson.* **1987**, *74*, 316.
(38) Rinkel, L. J.; Altona, C. *J. Biom. Struct. Dyn.* **1987**, *4*, 621.
(39) Boogaard, N.; Altona, C.; Reedijk, J. *J. Inorg. Biochem.* **1993**, *49*, 129.
(40) Kline, T. P.; Marzilli, L. G.; Live, D.; Zon, G. *J. Am. Chem. Soc.* **1989**, *111*, 7057.
(41) den Hartog, J. H. J.; Altona C.; Van der Marel, G. A.; Reedijk, J. *Eur. J. Biochem.* **1985**, *147*, 371.

relatively intense ROE H8/H8 cross-peaks observed in the 2D ROESY NMR spectrum (Figure 4). Among the minimized HH1 and HH2 conformers of the HH adducts (1 and 2 refer to models with 5′-G and 3′-G positioned to the left, respectively)[11] the lowest in energy are left-handed. This finding correlates with the 3′-G downfield and 5′-G upfield relationship of the H8 ^{1}H NMR resonances (Figure S2*; vide supra*), and points to the presence of an HH1 L conformer in solution, in good agreement with all the well characterized HH1 single-stranded (*ss*) d{(p)GpG} platinum adducts in solution being HH1 L.[25,34,44] However, the 1 kcal difference in energy between the lowest HH1 L and HH2 R conformers lends credence to the modeling studies performed by Kozelka *et al.* for *cis*-[Pt(NH$_3$)$_2$-{d(pGpG)}],[45] wherein it is suggested that the L- to R-canting for the cisplatin adduct requires only a small amount of energy. The equal number of L- and R-canted molecules in the solid state for *cis*-[Pt(NH$_3$)$_2${d(pGpG)}][3b] further supports this argument. The Rh$_2$(OAc)$_2${d(pGpG)} models exhibit a conformational change of the 5′-G sugar ring from the usual B-DNA S-(C2′-endo) to N-type (C3′-endo) pucker, whereas the 3′-G sugar ring remains C2′-endo; this structural change alleviates the strain induced by the destacking of the coordinated guanine bases. The structural features of the Rh$_2$(OAc)$_2${d(pGpG)} adduct, resulting from the molecular modeling, are in full agreement with those deduced from the ^{1}H NMR data, as well as with the crystal structure of *cis*-[Pt(NH$_3$)$_2${d(pGpG)}].[3b] To assess the similarities of Rh$_2$(OAc)$_2${d(pGpG)} to *cis*-[Pt(NH$_3$)$_2${d(pGpG)}], a comparison between 200 Rh$_2$(OAc)$_2${d(pGpG)} structures derived from simulated annealing calculations with that of the crystallographically determined *cis*-[Pt(NH$_3$)$_2${d(pGpG)}] adduct was undertaken. It was found that 10% of the Rh$_2$(OAc)$_2$-{d(pGpG)} structures have closely related conformations to that of the crystallographically determined *cis*-[Pt(NH$_3$)$_2${d(pGpG)}]. The superposition of 10% of the structures with that of the crystallographically independent left-handed molecule 2 of *cis*-[Pt(NH$_3$)$_2${d(pGpG)}][3b] is depicted in Figure 6A; if slight differences in the backbone are disregarded, an even larger number of structures compare well to the cisplatin adduct with respect to the position of the guanine bases. The superposition of the Rh$_2$(OAc)$_2${d(pGpG)} conformer (having an energy within 2 kcal/mol from the lowest energy structure) bearing the greatest resemblance to the crystallographically determined structure of *cis*-[Pt(NH$_3$)$_2${d(pGpG)}] with the latter is depicted in Figure 6B. Not only are the conformational features of the two adducts remarkably similar, but the bases are destacked to the same degree upon coordination to the metal (interbase dihedral angle 3′-G/5′-G = 81.3° and 80.6° for the minimized dirhodium conformer and the cisplatin crystal structure, respectively; Table 3), and favorably poised to accommodate the bidentate *N7/O6* binding to the rhodium centers.

The lowest energy conformers of the HH Rh$_2$(OAc)$_2$-{d(TGG)} adduct are left-handed, thereby confirming the recently proposed trend of the 5′-group steric effect[44] discussed in detail in the following section.

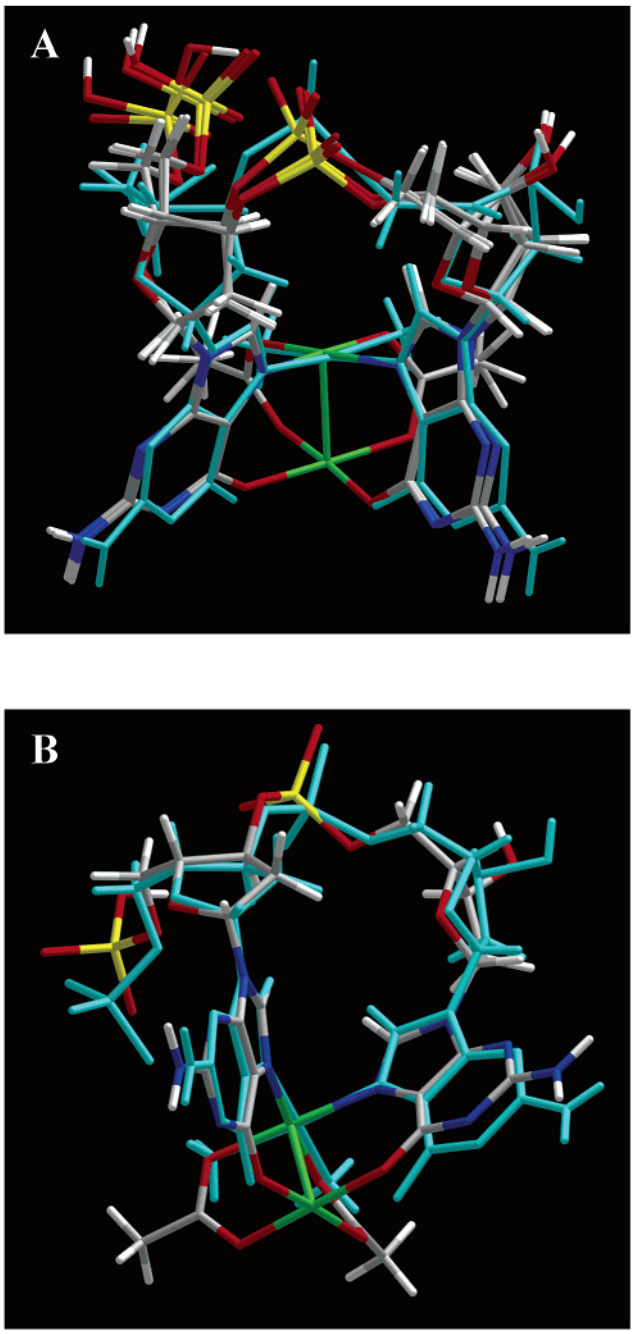

Figure 6. Superposition of the crystallographically determined *cis*-[Pt-(NH$_3$)$_2${d(pGpG)}][3b] (light blue) (left-handed molecule 2 from the unit cell which has four independent molecules) with (A) 20 HH1 L Rh$_2$(OAc)$_2$-{d(pGpG)} conformers (10% of the total structures resulting from simulated annealing calculations) that resemble closely the cisplatin adduct, and (B) the most similar HH1 L Rh$_2$(OAc)$_2${d(pGpG)} conformer. The 5′-G is depicted to the left. Color code for Rh$_2$(OAc)$_2${d(pGpG)}: Rh green, N dark blue, O red, P yellow, C gray, H white.

Discussion

N7/O6 Binding of the Dirhodium Adducts. The products of the reaction of 5′-GMP with Rh$_2$(OAc)$_4$ conform to the behavior of those of 9-EtGH[10,11] with the added effect of the 5′-phosphate group. In the ^{1}H NMR spectrum of the Rh$_2$(OAc)$_2$-(5′-GMP)$_2$ reaction solution, the presence of two isomers is evidenced by the two downfield shifted H8 resonances, in 1:0.8

(42) (a) Gellert, R. W.; Bau, R. *J. Am. Chem. Soc.* **1975**, *97*, 7379. (b) Cramer, R. E.; Dahlstrom, P. L. *J. Am. Chem. Soc.* **1979**, *101*, 3679. (c) Cramer, R. E.; Dahlstrom, P. L.; Seu, M. J. T.; Norton, T.; Kashiwagi, M. *Inorg. Chem.* **1980**, *19*, 148. (d) Barnham, K. J.; Bauer, C. J.; Djuran, M. I.; Mazid, M. A.; Rau, T.; Sadler, P. J. *Inorg. Chem.* **1995**, *34*, 2826.
(43) Saad, J. S.; Scarcia, T.; Shinozuka, K.; Natile, G.; Marzilli, L. G. *Inorg. Chem.* **2002**, *41*, 546.
(44) Sullivan, S. T.; Saad, J. S.; Fanizzi, F. P.; Marzilli, L. G. *J. Am. Chem. Soc.* **2002**, *124*, 1558.
(45) Kozelka, J.; Fouchet, M.-H.; Chottard, J.-C. *Eur. J. Biochem.* **1992**, *205*, 895.

ratio, favoring the HH isomer. The chemical shifts of the H8 protons for both adducts show pH-independent behavior at pH < 3.0 (Figure 1, curves A and B), a fact indicative of *N7* binding for purines. Furthermore, the *decreased* value of *N1−H* deprotonation for the HT isomer to p$K_a \approx 5.6$ (Figure 1, curve B), which is a value comparable to that of the 9-EtGH adduct(s) (p$K_a \approx 5.7$),[11] strongly suggests *O6* binding to the metal. For the HH isomer, the effect of *O6* binding on the ^{1}H NMR chemical shift of H8 is equal in magnitude but opposite in direction, to that of the 5′-phosphate group deprotonation occurring at a similar pH (Figure 1, curve A; the 5′-phosphate and the *N1* protonations induce up- and downfield shifts of the H8 ^{1}H NMR resonance, respectively).[20] The two effects of approximately equal magnitude result in a nearly pH-independent ^{1}H NMR H8 resonance titration curve for the HH isomer and cause its H8 proton to be more shielded than the H8 of the HT isomer at pH < 5.5 (Figure 1) where the two effects take place (in the 9-EtGH dirhodium isomers, the H8 of the HH isomer is slightly less shielded than the H8 of the HT isomer at all pH values).[11] The insensitivity of the HT $Rh_2(OAc)_2$(5′-GMP)$_2$ H8 proton to the 5′-phosphate deprotonation is not unprecedented, and is attributable to the large distance between the latter group and the H8 (Table S1).[22]

In the case of $Rh_2(OAc)_2${d(pGpG)}, the chemical shifts for both 5′- and 3′-G H8 protons are nearly pH independent (at low pH this feature is indicative of *N7* binding to the metal; Figure 2).[19,20] The lack of shifting for the 5′-G H8 resonance (Figure 2, curve B) conforms to the pattern exhibited by the HH $Rh_2(OAc)_2$(5′-GMP)$_2$ H8 resonance (Figure 1, curve A), which is shifted equally but in opposite directions, due to *O6* binding and 5′-phosphate group deprotonation occurring at similar pH values; if *O6* were not bound to the dirhodium core, the expected pK_a of *N1* (de)protonation would be ~8.5 (comparable to that of *cis*-[Pt(NH$_3$)$_2${d(pGpG)}])[20], and thus not balanced by the 5′-phosphate (de)protonation usually observed at p$K_a \approx 6.0$. The unexpected sensitivity of the chemical shift of the 3′-G H8 proton of $Rh_2(OAc)_2${d(pGpG)} to the 5′-phosphate group deprotonation (Figure 2, curve A), attributed to the proximity of the latter group to the H8 (as indicated by the low energy conformers of the adduct; Table S1) results in a small, although reproducible, downfield shift of the 3′-G H8 ^{1}H NMR resonance as in the case of the *cis*-[Pt(NH$_3$)$_2${d(pGpG)}] 3′-G H8.[20]

The *enhanced* acidity of *N1−H* afforded by the purine *O6* binding to the rhodium centers has been further probed by the pH dependence studies for the C6 and C2 ^{13}C NMR resonances of the dirhodium adducts (nucleus C6 is near the metalation site *O6* and the deprotonation position *N1−H*, whereas C2 is proximal to the latter only). Figures 3 and S3 show the comparison of the inflection points of *N1−H* (de)protonation derived from ^{13}C NMR data for $Rh_2(OAc)_2$(5′-GMP)$_2$ and $Rh_2(OAc)_2${d(pGpG)} with respect to the unbound ligands. In the δ (^{13}C) *vs* pH plots, the pK_a of the *N1−H* (de)protonation decreases from ~10.0 for the unbound ligand to ~5.7 for the dirhodium adducts. The pH dependence studies of the ^{13}C NMR resonances resulted in pK_a values for the *N1−H* (de)protonation comparable to those derived from the ^{1}H NMR H8 titration curves and argue strongly for *O6* binding to the dirhodium centers. Comparison of the C6 and C2 ^{13}C NMR resonances of the dirhodium adducts with the corresponding resonances of the unbound ligands at pH 8 (only the bound guanine bases are deprotonated at this pH) indicates substantial *downfield* shifts of $\Delta\delta \approx 11$ and 6 ppm, respectively (Table 1). For the dirhodium adducts, the ^{13}C NMR resonances of nuclei C5 and C8 are moderately affected by *N7/O6* coordination.

Conformational Characteristics of the $Rh_2(OAc)_2${d(pGpG)} Adduct. The 2D NMR spectroscopic data of the $Rh_2(OAc)_2${d(pGpG)} adduct in solution revealed HH arrangement of the bases,[11,32−34] in addition to the 3′-G H8 downfield and 5′-G H8 upfield resonance relationship; these features conform to the structures of *cis*-[Pt(NH$_3$)$_2${d(pGpG)}][45] and other platinum d(pGpG) adducts in solution,[25,26b,44] and lead to an HH1 L association of this variant. Although, *cis*-[Pt(NH$_3$)$_2${d(pGpG)}] has an equal population of HH1 R and HH1 L variants in the solid state[3b] (indicative of the small energy barrier between the two variants, as inferred from the molecular mechanics calculations by Kozelka *et al*.[45] in addition to the present simulated annealing calculations; Table 3) the 5′-phosphate group favors the HH1 L variant. The 5′-phosphate increases the canting (and thus the shielding) of the 5′-G, and it simultaneously has a deshielding effect on it.[33b,44] It has recently been postulated by Marzilli *et al*. that the degree of L canting of HH1 depends on the 5′-X group steric effect with the 5′-phosphate group inducing less canting than a 5′-X residue (*i.e.*, X may be T).[44] In contrast to the two major right-handed HH R variants of $Rh_2(OAc)_2${d(GpG)},[11] left canting is favored for the $Rh_2(OAc)_2${d(pGpG)} adduct, lending thus credence to the proposed steric effect of the 5′-phosphate group.[44] Hydrogen bonding between the 5′-phosphate group of d(pGpG) and the acetate oxygen atoms is not the driving force for the increase of the left canting, because all the $Rh_2(OAc)_2${d(pGpG)} minimized structures give rise to acetate(*O*)···*H*OP(phosphate) distances > 5.5 Å (except for one conformer with 4.5 Å); the previous observation confirms the postulation of Marzilli *et al.* that amine (or carrier ligand) hydrogen bonding is inconsequential to the preference of the HH1 L conformers in platinum *ss* DNA adducts.[44] Accordingly, molecular modeling results indicate that the left-handed variants of the $Rh_2(OAc)_2${d(TGG)} adduct are the most stable, in agreement with the previously mentioned arguments.

Salient features that emerged from the 2D NMR spectroscopic data of the $Rh_2(OAc)_2${d(pGpG)} adduct include *anti* orientation of the sugars with respect to the guanine bases and repuckering of the 5′-G sugar ring to C3′-endo (N-type) conformation. The aforementioned features bear close resemblance to those of *cis*-[Pt(NH$_3$)$_2${d((p)GpG)}], the latter known to exist as HH cross-linked adducts with *anti* oriented 5′-G and 3′-G sugar rings in the C3′-endo (N-type) and C2′-endo (S-type) conformations, respectively. Comparison of the low energy $Rh_2(OAc)_2${d(pGpG)} conformer with the crystal structure of *cis*-[Pt(NH$_3$)$_2${d(pGpG)}] depicted in Figure 6B, reveals remarkable similarities between the two adducts; not only are the bases almost completely destacked upon coordination to the metal in both cases, but they are favorably poised to accommodate the bidentate *N7/O6* binding to the rhodium centers. The rigid steric demands of the tethered guanine bases bound to the tetrahedral platinum atom in *cis*-[Pt(NH$_3$)$_2${d(pGpG)}], reflected by the 5′-G C3′-endo sugar ring conformation and *anti/anti* sugar orientation, are retained in the dirhodium adducts with bridging *N7*/*O6* tethered guanine bases; the interaction motif is similar

for both metal compounds which possess two *cis* positions available for covalent binding of the tethered guanine residues.

Conclusions

The unprecedented *N7/O6* equatorial binding of the guanine bases {as observed for the 9-EtGH and d(GpG) dirhodium compounds}[10,11] is conserved in the cases of the 5′-GMP and d(pGpG) dirhodium adducts. The tethering of the guanine bases governs the HH nature of the $Rh_2(OAc)_2${d(pGpG)} adduct, while the terminal 5′-phosphate group induces the stabilization of one left-handed HH1 L conformer in solution. It is well documented that platinum-GG cross-links are left-handed in *ss* DNA and right-handed in duplexes, but the factors contributing to the difference in canting are poorly understood. The HH R to HH L conversion of the dirhodium adduct, attributed to the addition of the 5′-phosphate group to the d(GpG) dinucleotide, accords with the reported *steric* effect of the 5′-group which favors left canting.[44]

The remarkable similarities between $Rh_2(OAc)_2${d(pGpG)} and the crystallographically determined *cis*-[$Pt(NH_3)_2${d(pGpG)}] adducts imply that the 90° bite angle displayed by the d(pGpG) "chelate" ligand in the cisplatin intrastrand adduct is well suited to also bind at two *cis* equatorial positions of one rhodium center in a dinuclear complex. The unequivocal finding that the d(pGpG) DNA fragment can bind equatorially to the dirhodium unit via *N7*/*O6* bridges spanning the Rh−Rh bond raises thus the possibility that such binding modes to DNA may be involved in the antitumor activity of dinuclear metal carboxylate and related compounds.

The loss of stacking in the coordinated bases and the resulting bend in the double helix, induced by the steric demands of the bifunctional binding of DNA to *cis*-DDP, are features recognized by HMG domain and other proteins.[2c,5a] It remains to be determined if these alterations in the helical structure are maintained in the dirhodium adducts with double-stranded DNA.

Acknowledgment. Professor Jan Reedijk is gratefully acknowledged for stimulating discussions and critical suggestions. Professor Andy Li-Wang and Dr. Doug A. Klewer are kindly acknowledged for helpful discussions. Dr. Steven K. Silber and Dr. Michael Angel provided valuable technical assistance with the ^{13}C NMR data collection. Dr. David Young is gratefully acknowledged for preliminary work on the molecular modeling studies. The authors thank the reviewers for helpful comments. The Laboratory for Molecular Simulation at Texas A&M University is acknowledged for providing software and computer time. Use of the TAMU/LBMS-Applications Laboratory (Laboratory of Biological Mass Spectroscopy) and Dr. John M. Koomen are also acknowledged. K.R.D. thanks Johnson-Matthey for a generous loan of dirhodium tetraacetate. The NMR instrumentation in the Chemistry Department at Texas A&M University was funded by NSF (CHE-0077917). The NMR instrumentation in the Biomolecular NMR Laborartory at Texas A&M University was supported by a grant from the National Science Foundation (DBI-9970232) and the Texas A&M University System. K.R.D. thanks the State of Texas for an ARP grant (010366-0277-1999), and the Welch Foundation (A1449) for financial support. H.T.C. thanks NATO for a postdoctoral fellowship during the initial stages of this work.

Supporting Information Available: Table with selected distances for the dirhodium bis-acetate adducts; table with calculated energies and experimentally observed percent of dirhodium bis-acetate adducts; figures of pH dependence of the 5′-phosphate ^{31}P NMR resonances for the HH and HT $Rh_2(OAc)_2(GMP)_2$ isomers in D_2O at 20 °C; aromatic region of 1D ^1H NMR spectrum of $Rh_2(OAc)_2${d(pGpG)} in D_2O at 20 °C, pH 7.8; pH dependence of the ^{13}C NMR resonances for nuclei C6 and C2 of $Rh_2(OAc)_2${d(pGpG)} and unbound d(pGpG) in D_2O at 20 °C; H1′ and H2′/H2″ regions of the 2D [^1H-^1H] DQF-COSY NMR spectrum of $Rh_2(OAc)_2${d(pGpG)} in D_2O at 20 °C, pH 7.8; temperature dependence of the ^{31}P NMR resonances of the phosphate mono- and diester groups for $Rh_2(OAc)_2${d(pGpG)} in D_2O at pH 6.5; MALDI spectrum of $Rh_2(OAc)_2${d(pGpG)}. This material is available free of charge via the Internet at http://pubs.acs.org.

JA0291585